ECCM-2001
European Conference on
Computational Mechanics
June 26-29, 2001
Cracow, Poland

NONLINEAR FINITE ELEMENT ANALYSIS OF RESIDUAL STRESSES IN SEMICONDUCTOR EPILAYERS

Paweł Dłużewski * **and Grzegorz Maciejewski**
Institute of Fundamental Technological Research PAS,
Świętokrzyska 21, 00-049 Warsaw
e–mail: pdluzew@ippt.gov.pl

Sławomir Kret
Institute of Physics PAS,
Al. Lotników 32/46, 02-668Warsaw

Key words: Dislocations, Residual Stresses, Heteroepitaxial layers

Abstract. *By digital image processing based on the geometric phase method a lattice distortion field of GaAs/ZnTe/CdTe epilayer is reconstructed from HRTEM micrograph. The field is used next as input data to finite element code. A nonlinear elastic-plastic finite element algorithm is developed to predict the residual stress distribution induced by misfit dislocations in semiconductor heteroepitaxial layers. In the approach developed the important role takes elastic nonlinearity. The third-order elastic constants, usually determined experimentally in relation to the Green strain, are recalculated here to the logarithmic strain. Attention is also given to the modelling of elastic properties of dislocations. Paper shows numerical results obtained by means of the nonlinear finite element method.*

1 Introduction

Recently, computer methods used to digital image processing of images obtained from the high-resolution transmission electron microscopy (HRTEM) allows a quantitative measurement of lattice distortions in the atomic scale, [3, 4]. One of them we use to determine the lattice distortions in the CdTe/ZnTe/GaAs heterostructure. The stress distribution in heterostructure depends not only on lattice distortion, but also on the local chemical composition. The elastic strains can reach only a few percents, while the chemical strains induced by the chemical composition can take a several percents, e.g. in CdTe/ZnTe/GaAs layers discussed below the chemical strain of lattice between GaAs base and CdTe layer overcome 14%. On the other hand in the linear theory of elasticity the strains corresponding to stress ranged 1 GPa does not exceed a few percent. Therefore, to accommodate the chemical distortion changes from layer to layer the strongly dislocated interfacial regions come into existence between layers.

The finite element (FE) method is rarely employed to predict the residual stress distribution induced by dislocations. The reason of that yields from difficulties in finding the suitable numerical algorithms based upon the displacement field method being the foundation of the most of FE codes (the dislocation distribution tensor field is not integrable). The semi-numerical methods based upon analytical solutions obtained from the linear theory of elasticity is one of possible solution of this problem, see e.g. the strain distribution in the finite element technique used by Stigh [5]. In the present paper we propose another, purely numerical method. Anisotropic hyperelastic materials compose a narrow group among numerous constitutive models describing elastic behaviour of solids. It is worth emphasizing that the most known *anisotropic* hyperelastic models like the St-Venant–Kirchhoff model change strongly their (instantaneous) stiffness under large strains. Moreover, this stiffness evolution differs significantly for compression region (increases) and tension region (decreases) this phenomenon manifests by

- the bending of epitaxial layers induced by misfit dislocations [1],
- the dependence of elastic stiffness on hydrostatic pressure,
- negative values of third-order elastic constants measured for many crystal structures [2].

Therefore, the analysis of nonlinear elastic properties takes fundamental role in the estimation of stress distribution in epitaxial layers, as well as, in many other problems, e.g. in prediction of the elastic-plastic instability where the correct estimation of the instantaneous stiffness of extremely deformed materials takes the important role. The use of new elastic and elastic-plastic constitutive models which behaviour could be more adapted to the nonlinear behaviour of real crystal structures is to be desired.

2 The lattice distortions

A typical high quality image of GaAs/ZnTe/CdTe interface in the [110] projection is shown in Fig. 1. Contrast in GaAs and CdTe is homogeneous – bright dots on dark background. The

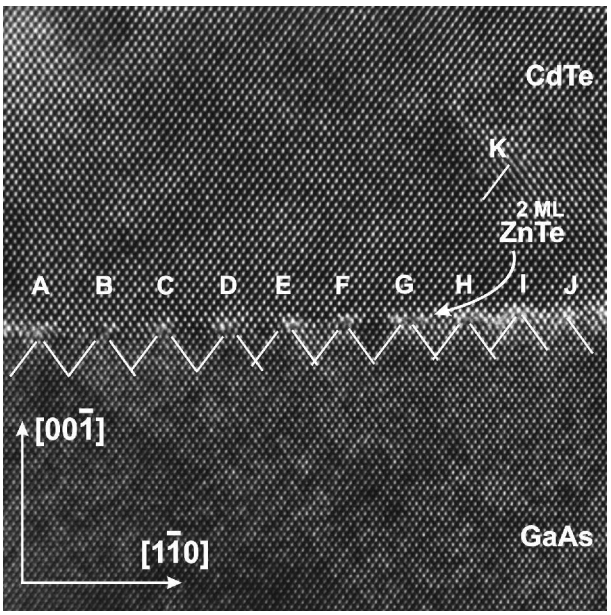

Figure 1: HRTEM image of the considered heterostructure.

interface (substrate surface) is tilted of about 2° relatively to crystallographic directions. So, 4 mono-atomic steps appears between the left and right border of image. Their hypothetical positions have been marked by horizontal segment lines in Fig. 1. CdTe and GaAs layers take the same sphalerite structure with lattice mismatch 14.6%. Nine per ten misfit dislocations visible on the interface are the edge Lomer dislocations. Their Burgers vectors take components $\frac{1}{2}[1\bar{1}0]$. The dislocation lines are parallel to the interfacial plane and perpendicular to the electron beam. Only one 60° dislocation is visible on interface, see dislocation J. Its Burgers vector takes components $\frac{1}{2}[0\bar{1}\bar{1}]$ or $\frac{1}{2}[10\bar{1}]$ and is deviated at 60° from its dislocation line being parallel to electron beam and laying in $(1\bar{1}1)$ plane. The second 60° dislocation is situated 8 nm upper interface, see dislocation K. The next dislocations (invisible in Fig. 1) was found far away from the interface (20-25nm). The visible Lomer dislocations can be interpreted as two clearly separated 60° elemental dislocations. By means of a geometric phase method the distribution of lattice distortions can be reconstructed from HRTEM image. This method is based upon centering a small aperture around a strong reflection in the Fourier transform of image, see details in [3, 4]. The phase component of the resulting complex image gives information about local displacements of atomic planes. Applying two non-collinear Fourier components a two-dimensional piecewise continuous displacement field $\widehat{\mathbf{u}}(\mathbf{x})$ has been determined. Differentiating the displacement field a continuous field of lattice distortions $\beta(\mathbf{x})$ is reconstructed. Obviously, in the heterostructure like GaAs/ZnTe/CdTe the lattice distortions results not only from the elastic but also from the chemical distortions induced by changes in composition of crystal lattice. Therefore, in our case, the lattice distortions have been determined in relation to a fixed local reference configuration assumed for the whole heterostructure and corresponding to a perfect GaAs lattice. More details on determination of this distortion field are given by Kret *et al.* [6].

3 Deformation description

In this paper a motion of crystal lattice in the three-dimensional positively oriented Euclidean space E^3 is described in terms of the nonlinear continuum mechanics. Traditionally, the current position of given particles is described by three co-ordinates x^1, x^2, x^3 determined in an immobile curvilinear coordination set $\{x^k\}$, while the reference position $\mathbf{X}$ is represented by three other coordinates X^1, X^2, X^3 determined in other immobile coordinate set $\{X^K\}$. Then the components of deformation gradient are determined as

$$F^k{}_K = \frac{\partial x^k}{\partial X^K}. \tag{1}$$

In terms of the absolute notation the deformation gradient is determined as

$$\mathbf{F} = \frac{\partial \mathbf{x}}{\partial \mathbf{X}}. \tag{2}$$

It is convenient to distinguish the lattice deformation from the total deformation gradient. So, let us assume a multiplicative decomposition

$$\mathbf{F} = \mathbf{F}_{\mathrm{lt}}\mathbf{F}_{\mathrm{pl}}, \tag{3}$$

where $\mathbf{F}$ denotes the so-called total deformation gradient, $\mathbf{F}_{\mathrm{lt}}$ is the lattice deformation gradient while $\mathbf{F}_{\mathrm{pl}}$ denotes a remnant resulting from the (permanent) rearrangement of atoms composing the crystal lattice. The above deformation tensors can be considered in terms of displacement deformation gradients

$$\mathbf{F} = \frac{\partial \mathbf{x}}{\partial \mathbf{X}} = \mathbf{1} - \frac{\partial \mathbf{u}}{\partial \mathbf{X}}, \tag{4}$$

$$\mathbf{F}_{\mathrm{lt}} = \frac{\partial \mathbf{x}}{\partial \widehat{\mathbf{x}}} = \mathbf{1} - \frac{\partial \widehat{\mathbf{u}}}{\partial \widehat{\mathbf{x}}}, \tag{5}$$

$$\mathbf{F}_{\mathrm{pl}} = \frac{\partial \widehat{\mathbf{x}}}{\partial \mathbf{X}} = \mathbf{1} - \frac{\partial (\mathbf{u} - \widehat{\mathbf{u}})}{\partial \mathbf{X}}, \tag{6}$$

where $\widehat{\mathbf{x}}$ denotes the reference position in the lattice reference configuration while $\mathbf{x}$ and $\mathbf{X}$ denote the position in the actual and material reference configuration, respectively.

The spatial gradient of the lattice displacement field $\widehat{\mathbf{u}}(\mathbf{x})$ can be rewritten in relation to the gradient referred to lattice reference configuration according to local differential relation e.g.

$$\frac{\partial \widehat{\mathbf{u}}}{\partial \widehat{\mathbf{x}}} = \left(\mathbf{1} - \frac{\partial \widehat{\mathbf{u}}}{\partial \mathbf{x}}\right)^{-1} - \mathbf{1}. \tag{7}$$

Substituting (7) into (5) we note that

$$\mathbf{F}_{\mathrm{lt}} = (\mathbf{1} - \boldsymbol{\beta})^{-1}. \tag{8}$$

3.1 Continuum description of dislocation distribution

The dislocation distribution measures are dependent on the lattice distortion gradient. The geometric meaning of dislocation distribution tensors can be formulated drawing the respective Burgers circuit in the current or in the lattice reference configuration, cf. the FS/RH and SF/RH methods described by Hirth [7]. The first of them consists in drawing a closed circle in the actual configuration and finding the Burgers vector in the reference one. In the continuum theory of dislocations according to the SF/RH method we find the following relation

$$\widehat{\mathbf{b}} = \int_C \mathbf{F}_{\mathrm{lt}}^{-1} d\mathbf{x} = \int_{S_C} \operatorname{curl} \mathbf{F}_{\mathrm{lt}}^{-1} d\mathbf{s} = \int_{S_C} \widetilde{\boldsymbol{\alpha}} d\mathbf{s}, \tag{9}$$

where the distribution of the true Burgers vector in the current configuration is described by the following tensor

$$\widetilde{\boldsymbol{\alpha}} \stackrel{df}{=} \operatorname{curl} \mathbf{F}_{\mathrm{lt}}^{-1}. \tag{10}$$

The true Burgers vector specifies the crystallographic components of dislocations referred to undeformed crystal lattice. The area elements and differential forms of Burgers vectors satisfy the well-known transformation rules

$$d\mathbf{b} = \mathbf{F}_{\mathrm{lt}}\, d\widehat{\mathbf{b}}, \tag{11}$$

$$d\mathbf{s} = \mathbf{F}_{\mathrm{lt}}^{-T} d\widehat{\mathbf{s}}\, \det \mathbf{F}_{\mathrm{lt}}. \tag{12}$$

Substitution them into the differential form of (9) gives the following differential relations

$$d\mathbf{b} = \boldsymbol{\alpha} d\mathbf{s} \qquad \text{and} \qquad d\widehat{\mathbf{b}} = \widehat{\boldsymbol{\alpha}} d\widehat{\mathbf{s}}, \tag{13}$$

where

$$\boldsymbol{\alpha} \stackrel{df}{=} \mathbf{F}_{\mathrm{lt}} \operatorname{curl} \mathbf{F}_{\mathrm{lt}}^{-1} \qquad \text{and} \qquad \widehat{\boldsymbol{\alpha}} \stackrel{df}{=} \operatorname{curl} \mathbf{F}_{\mathrm{lt}}{}^{-1} \mathbf{F}_{\mathrm{lt}}^{-T} \det \mathbf{F}_{\mathrm{lt}}, \tag{14}$$

cf. (10); $\boldsymbol{\alpha}$ represents the distribution of spatial Burgers vector while $\widehat{\boldsymbol{\alpha}}$ specifies the distribution of the true Burgers vector referred to the lattice reference configuration. With respect to compatibility condition, which have to be satisfied between the plastic and lattice distortion tensors, it can be proved that the above tensorial measures of dislocations can be rewritten using many mutually different derivatives.

On this base we find the following formulas equivalent to definitions (14), see [8, 9],

$$\boldsymbol{\alpha} = \operatorname{grad} \mathbf{F}_{\mathrm{lt}} \mathbin{\dot{\times}} \mathbf{F}_{\mathrm{lt}}^{-1} \tag{15}$$

$$= \mathbf{F}_{\mathrm{lt}} \mathbf{F}_{\mathrm{pl}} \operatorname{grad} \mathbf{F}_{\mathrm{pl}}^{-1} \mathbin{\dot{\times}} \mathbf{F}_{\mathrm{lt}}^{-1} \tag{16}$$

$$= -\mathbf{F}_{\mathrm{lt}} \operatorname{grad} \mathbf{F}_{\mathrm{pl}} \mathbin{\dot{\times}} (\mathbf{F}_{\mathrm{lt}} \mathbf{F}_{\mathrm{pl}})^{-1}, \tag{17}$$

$$\widehat{\boldsymbol{\alpha}} = -\operatorname{Grad} \mathbf{F}_{\mathrm{lt}}{}^{-1} \mathbin{\dot{\times}} \mathbf{F}_{\mathrm{lt}} \tag{18}$$

$$= -\mathbf{F}_{\mathrm{lt}}^{-1} \operatorname{Curl} \mathbf{F}_{\mathrm{lt}} \tag{19}$$

$$= -\mathbf{F}_{\mathrm{pl}} \operatorname{Curl} \mathbf{F}_{\mathrm{p}}^{-1} \tag{20}$$

$$= -\operatorname{Grad} \mathbf{F}_{\mathrm{pl}} \mathbin{\dot{\times}} \mathbf{F}_{\mathrm{pl}}^{-1} \tag{21}$$

$$= \operatorname{CURL} \mathbf{F}_{\mathrm{pl}}\, \mathbf{F}_{\mathrm{pl}}^{T} \det \mathbf{F}_{\mathrm{pl}}^{-1}. \tag{22}$$

In the numerical code presented in Section 5 the fundamental role takes relation (22).

Summing up our considerations on heterostructural deformations we assume the following decomposition of the total deformation gradient

$$\boxed{\mathbf{F} = \overbrace{\underbrace{\mathbf{R}\mathbf{U}}_{\mathbf{F}_{\mathrm{lt}}}\mathbf{F}_{\mathrm{ch}}}^{\mathbf{F}_{\mathrm{lt}'}}\mathbf{F}_{\mathrm{pl}},} \tag{23}$$

where $\mathbf{R}$ and $\mathbf{U}$ denotes the rotation and stretch of the actual crystal structure determined in relation to its stress-free configurations, while $\mathbf{F}_{\mathrm{ch}}$ denotes the chemical deformation between two stress-free configurations differing the chemical composition, namely, between the actual (e.g. CdTe) and the reference chemical compositions (GaAs).

4 Nonlinear elasticity

According to the polar decomposition theorem the deformation gradient $\mathbf{F}$ can be decomposed into the rotation tensor $\mathbf{R}$ and into the left or right stretch tensor, $\mathbf{U}$ or $\mathbf{V}$, respectively, $\mathbf{F} = \mathbf{R}\mathbf{U} = \mathbf{V}\mathbf{R}$. It can be proved, see [10, 11] that to balance energy for arbitrarily chosen deformation process the Cauchy stress has to be governed by the following equation

$$\boxed{\boldsymbol{\sigma} = \mathbf{R}(\widehat{\boldsymbol{\mathcal{A}}} : \widehat{\rho}\frac{\partial\psi}{\partial\widehat{\boldsymbol{\varepsilon}}})\mathbf{R}^T \det\mathbf{F}^{-1}.} \tag{24}$$

where the fourth-order tensor $\widehat{\boldsymbol{\mathcal{A}}}$ decomposed in the right stretch eigenvector basis $\{\mathbf{u}_{\mathsf{K}}\}$ is represented by the following non-vanishing components

$$\widehat{\mathcal{A}}_{\mathsf{IJIJ}} = \widehat{\mathcal{A}}_{\mathsf{IJJI}} = \begin{cases} \delta_{\mathsf{IJ}}\, u_{\mathsf{I}} f'(u_{\mathsf{I}}) & \text{for } u_{\mathsf{I}} = u_{\mathsf{J}}, \\ \frac{2u_{\mathsf{I}}u_{\mathsf{J}}[f(u_{\mathsf{I}}) - f(u_{\mathsf{J}})]}{u_{\mathsf{I}}^2 - u_{\mathsf{J}}^2} & \text{for } u_{\mathsf{I}} \neq u_{\mathsf{J}}, \end{cases} \tag{25}$$

where $\widehat{\rho} = \rho \det\mathbf{F}$, $f'(u_{\mathsf{I}}) = \frac{df(u)}{du}\big|_{u=u_{\mathsf{I}}}$. Let us consider the hyperelastic material governed by the following constitutive equation stated for the specific internal energy

$$\psi = \psi(\widehat{\boldsymbol{\varepsilon}}, \widehat{\boldsymbol{\alpha}})|_{x_1,\ldots,x_n,T=\text{const}}, \tag{26}$$

where

$$\widehat{\boldsymbol{\varepsilon}} = \widehat{\boldsymbol{\varepsilon}}(\mathbf{F}_{\mathrm{lt}'}), \qquad \widehat{\boldsymbol{\alpha}} = \widehat{\boldsymbol{\alpha}}(\mathbf{F}_{\mathrm{lt}'}, \operatorname{grad}\mathbf{F}_{\mathrm{lt}'}) \qquad \text{and} \qquad \mathbf{F}_{\mathrm{lt}'} = \mathbf{F}_{\mathrm{lt}}\mathbf{F}_{\mathrm{ch}}^{-1}. \tag{27}$$

Third-order elastic constants are determinable by measurement of small changes of ultrasonic wave velocities in stressed crystals. Usually, they are determined for the constitutive relation between the second Piola-Kirchhoff stress and the Green strain called also the Lagrangian strain, see [13, 14, 15] among many others. So, let us assume here that a hyperelastic material satisfies the following specific strain energy function

$$\psi(\widehat{\boldsymbol{\varepsilon}}) = \frac{1}{\widehat{\rho}}\left[\frac{1}{2!}\widehat{c}^{ijkl}\widehat{\varepsilon}_{ij}\widehat{\varepsilon}_{kl} + \frac{1}{3!}\widehat{C}^{ijklmn}\widehat{\varepsilon}_{ij}\widehat{\varepsilon}_{kl}\widehat{\varepsilon}_{mn}\right], \tag{28}$$

where $\widehat{\mathrm{c}}$ and $\widehat{\mathrm{C}}$ are tensors of the second- and third-order elastic constants determined in relation to a given strain measure, for example let $m = 2$, what corresponds $\widehat{\boldsymbol{\varepsilon}} = \frac{1}{2}(\mathbf{U}^2 - \mathbf{1})$. By using the third-order elastic constants determined experimentally with respect to the Green strain ($m = 2$) by [15, 16] we find the third-order elastic constants related to the logarithmic strain ($m = 0$), see [10].

Additionally, in order to reduce the elastic stress carried out by dislocation cores we assume a constitutive equation which predicts the stiffness reduction in lattice disordered regions according to the following constitutive equation

$$\boldsymbol{\sigma} = \mathbf{R}\Big[\widehat{\boldsymbol{\mathcal{A}}} : (\widehat{\mathbf{c}}_\alpha : \widehat{\boldsymbol{\varepsilon}} + \frac{1}{2}\widehat{\boldsymbol{\varepsilon}} : \widehat{\mathbf{C}}_\alpha : \widehat{\boldsymbol{\varepsilon}})\Big]\mathbf{R}^T \det \mathbf{F}^{-1}, \tag{29}$$

where $\widehat{\boldsymbol{\varepsilon}}$ is the logarithmic strain, and

$$\widehat{\mathbf{c}}_\alpha = e^{-r\alpha}\widehat{\mathbf{c}} \tag{30}$$

$$\widehat{\mathbf{C}}_\alpha = e^{-2r\alpha}\widehat{\mathbf{C}}, \tag{31}$$

r is a dislocation core factor reducing the elastic stiffness in lattice disordered regions, α is assumed to be an invariant of the true dislocation distribution tensor allowing the computer recognition of dislocation core region in computational process.

In our 2D boundary-value plane problem discussed bellow the lattice disordered regions are recognized by using the following plain invariant of the dislocation distribution tensor

$$\alpha = \sqrt{\widehat{\alpha}_{\mathsf{xz}}^2 + \widehat{\alpha}_{\mathsf{yz}}^2}. \tag{32}$$

Using the continuized lattice distortion field the mentioned regions give strongly localized peaks on dislocation distribution tensor field. Outside the peaks the field $\widehat{\boldsymbol{\alpha}}(\mathbf{x})$ takes a value zero. The parameter r influences on the stiffness reduction in dislocation core regions.

5 Finite element analysis

We assume that the CdTe/ZnTe/GaAs lattice configuration visible in the HRTEM image in Fig. 2 is the *material reference* configuration of crystal lattice in relation to which the movement of material will be described. On the other hand, by a *lattice reference* configuration we mean a perfect GaAs lattice structure. Using the geometric phase method the dislocation distribution tensor field has been reconstructed from the image, see Fig. 2.

The following decomposition of the total deformation gradient is assumed

$$\mathbf{F} = \mathbf{F}_{\mathrm{lt}'}\mathbf{F}_{\mathrm{ch}}\mathbf{F}_{\mathrm{pl}}, \tag{33}$$

where $\mathbf{F}_{\mathrm{pl}}$ is the initial deformation tensor rebuilding (transforming) the lattice reference GaAs perfect structure to the dislocated heterostructure visible in HRTEM image. The perfect GaAs structure is identified here with a regular lattice visible considerably below the interface visible

on HRTEM image in Fig. 2. $\mathbf{F}_{\mathrm{lt}'} = \mathbf{RU}$ describes the lattice rotation and stretch measured in relation to a stress free configuration with the actual chemical composition. The chemical deformation tensor $\mathbf{F}_{\mathrm{ch}}$ describes the difference between two stress free configurations, namely with the actual chemical composition (e.g. CdTe) and with the reference chemical decomposition (GaAs). In our case $\mathbf{F}_{\mathrm{ch}}(\mathbf{x}) = \frac{\widehat{a}(\mathbf{x})}{\widehat{a}_{\mathrm{GaAs}}}$, where $\widehat{a}$ and $\widehat{a}_{\mathrm{GaAs}}$ denote the lattice cell parameter taken in two stress-free configurations mentioned above.

The initial and total deformation gradients are related to the source lattice distortion $\boldsymbol{\beta}_{\mathrm{HRTEM}}$ and to the material displacement vector $\mathbf{u}$ by the following relations

$$\mathbf{F}^{-1} = \mathbf{1} - \nabla\mathbf{u} = \frac{\partial(\mathbf{x} - \mathbf{u})}{\partial\mathbf{x}} = \frac{\partial\mathbf{x}_{\mathrm{HRTEM}}}{\partial\mathbf{x}}, \tag{34}$$

$$\mathbf{F}_{\mathrm{pl}} = \mathbf{1} + \boldsymbol{\beta}_{\mathrm{HRTEM}} = \frac{\partial(\widehat{\mathbf{x}} + \widehat{\mathbf{u}})}{\partial\widehat{\mathbf{x}}} = \frac{\partial\mathbf{x}_{\mathrm{HRTEM}}}{\partial\widehat{\mathbf{x}}}, \tag{35}$$

where

$$\mathbf{x} = \mathbf{x}_{\mathrm{HRTEM}} + \mathbf{u}, \qquad \mathbf{x}_{\mathrm{HRTEM}} = \widehat{\mathbf{x}} + \widehat{\mathbf{u}} \qquad \text{and} \qquad \boldsymbol{\beta}_{\mathrm{HRTEM}} = \frac{\partial\widehat{\mathbf{u}}}{\partial\mathbf{x}_{\mathrm{HRTEM}}}, \tag{36}$$

So, the position $\mathbf{x}$ and lattice distortion $\boldsymbol{\beta}$ iterated in FEM are determined by the following relations

$$\mathbf{x} = \mathbf{u} + \mathbf{X}^{\mathrm{HRTEM}}, \tag{37}$$

$$\boldsymbol{\beta} = \mathbf{1} - (\mathbf{1} - \boldsymbol{\beta}^{\mathrm{HRTEM}})^{-1}(\mathbf{1} - \nabla\mathbf{u}). \tag{38}$$

So, we find

$$\mathbf{F}_{\mathrm{lt}'}^{-1} = \mathbf{F}_{\mathrm{ch}}\mathbf{F}_{\mathrm{pl}}(\mathbf{1} - \nabla\mathbf{u}). \tag{39}$$

The equilibrium configuration iterated in FEM differs from the HRTEM image configuration. Among others this is because of in our numerical algorithm both the boundary condition, stress-strain behaviour, as well as chemical composition slightly differ from those corresponding to the HRTEM investigations. Therefore taking into account the geometry of dislocated structure from HRTEM image we assume: a fictitious stress-free boundary, a hypothetical chemical composition having a conviction that it is very close to the real composition as well as we assume a hypothetical stress-strain constitutive equation which should describe as close as possible for us the behaviour of the observed structure. For instance we assume a stress free boundary conditions to determine the residual stress stored in the analysed region of heterostructure. Our algorithm is based on a FE integration of the equilibrium equation in the *current* configuration, [17, 18], i.e.

$$\mathrm{div}\,\boldsymbol{\sigma} = \mathbf{0} \tag{40}$$

where, according to the previously discussed constitutive equations, the Cauchy stress tensor is a nonlinear function of $\mathbf{u}, \nabla\mathbf{u}, \boldsymbol{\beta}^{\mathrm{HRTEM}}$. Applying the virtual work principle we find the following nonlinear matrix equation

$$\mathbf{P}(\mathbf{a}) = \mathbf{f}, \tag{41}$$

where

$$\mathbf{P} = \left[\begin{array}{c} \int_v \nabla^T \mathbf{W}\boldsymbol{\sigma}\, dv \\ \mathbf{0} \end{array} \right], \quad \mathbf{a} = \left[\begin{array}{c} \mathbf{u} \\ \boldsymbol{\beta}_{\mathrm{HRTEM}} \end{array} \right], \quad \mathbf{f} = \left[\begin{array}{c} \int_{\partial v} \mathbf{W}\boldsymbol{\sigma}\, d\mathbf{s} \\ \mathbf{0} \end{array} \right]. \tag{42}$$

$\mathbf{W}$ denotes the weighting function determined in relation to the current (iterated) configuration. In the interior of finite elements the distribution of displacement field is governed by the relation

$$\mathbf{u}(\mathbf{x}) = \sum_{\mathsf{i}=1,9} N^u_{\mathsf{i}}(\mathbf{x})\, \mathbf{u}_{\mathsf{i}} \tag{43}$$

$$\boldsymbol{\beta}^{\mathrm{HRTEM}}(\mathbf{x}) = \sum_{\mathsf{i}=1,4} N^{\beta}_{\mathsf{i}}(\mathbf{x})\, \boldsymbol{\beta}^{\mathrm{HRTEM}}_{\mathsf{i}}. \tag{44}$$

We have applied the 9-node shape function for displacements N^{u} and 4-node function for initial distortions $\boldsymbol{\beta}^{\mathrm{HRTEM}}$. Fixing deformation freedom degrees corresponding to the lower part of the matrix equation (41) *its upper part was solved only*! Such a technique (with an undetermined lower part and solvable upper part for fixed lower variable $\boldsymbol{\beta}^{\mathrm{HRTEM}}_{\mathsf{i}}$) has been applied in order to obtain continuous, differentiable and mutually compatible fields $\mathbf{u}(\mathbf{x})$, $\mathbf{F}_{\mathrm{lt}}(\mathbf{x})$ and $\widehat{\boldsymbol{\alpha}}(\mathbf{x})$. The approach described above have been implemented as a user element to the FEAP program v. 7.1f. The upper part of the nonsymmetric equation set (41) was solved by using the Newton-Raphson method. In our case the tangent stiffness matrix takes the form $\mathbf{K} = \frac{\partial \mathbf{P}}{\partial \mathbf{a}}$ what gives

$$K_{\mathsf{ij}} = \int_v \nabla N_{\mathsf{i}} \frac{\partial(\boldsymbol{\sigma}\, \det \mathbf{F})}{\partial \mathbf{a}_{\mathsf{j}}} \det \mathbf{F}^{-1} dv. \tag{45}$$

5.1 Numerical example

Below, a plane boundary-value problem of the residual stress distribution induced by dislocations shown in Fig. 2 is described. This simplified (2D) problem is treated here as a numerical test for the mathematical algorithm presented above. The whole HRTEM image was recorded in the form of 1024×1024 bitmap. Due to some boundary errors obtained by image processing in the Fourier space, a boundary zone has been excluded from the stress analysis. So, after rejecting a 30 pixel wide zone per edge of the image its central region was taken into FE analysis, 964px×964px. This region was divided next into 100×100 = 10 000 ninth-node square elements.

The nodal values of the source distortion field $\beta_{\mathrm{HRTEM}\,\mathsf{i}}$ was obtained by averaging the distortions over all pixels situated near the node. Thus, each of elements occupied 9px×9px in the reference (HRTEM) configuration what meant that each element occupied the region $\frac{1}{2}\widehat{a}_{\mathrm{GaAs}} \times \frac{2}{3}\widehat{a}_{\mathrm{GaAs}}$.

6 Conclusions

Solving the boundary-value problem discussed above we have obtained the stress distribution shown in Fig. 2. The obtained stress distribution depends very strongly on the assumed lattice parameters. It is visible that the relaxed configuration demonstrate a small volume expansion

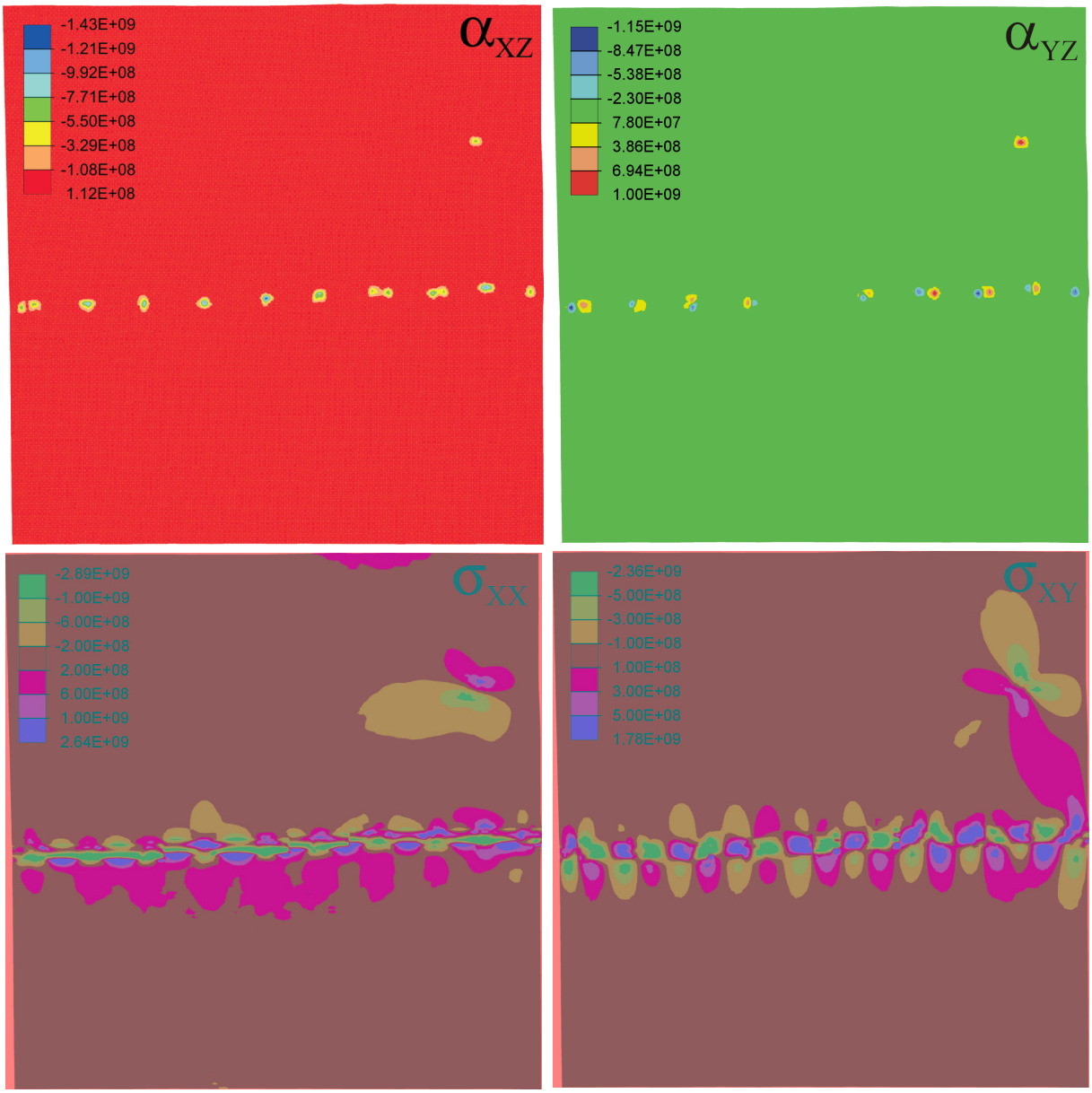

Figure 2: Dislocation and stress distribution obtained for considered CdTe/ZnTe/GaAs epilayer.

in relation to the initial one. From the experimental point of view it is generally known that a single dislocation induces a local volume expansion in crystal lattice. This expansion reach often a value about $1.0\,b^2$ per unit length of dislocation in the bulk crystal. On the other hand, from the viewpoint of the nonlinear theory of elasticity this effect can be observed only if the elastic material becomes harden for compression and soften for tension. Then the more rigid compressed part changes volume smaller than more flexible part expands caring out the most of misfit deformation needed to hold the lattice continuity about dislocations. Because the most of real crystals become harden for compression and soften for extension therefore the misfit dislocations situated on interfaces induce locally a volume expansion at the same time all lattice cells situated between dislocations are undergone a strong elastic compression. In result the whole interlayer tends to surface expansion. This nonlinear elastic effect is often incorporated to the linear elastic theory by assuming an additional surface tension.

Nonlinear equations of elasticity proposed here make the compression harden and extension soften. Therefore in our numerical solution the dislocations demonstrate some volume expansion. So, contrary to the linear theory we have not a reason to assume a surface tension additionally. Obviously, in our case, the crucial problem is how far the higher order elastic constants used give possibility for fitting our constitutive model to the nonlinear elastic behaviour of real crystal lattice. Nevertheless, one of the fundamental advantage of the presented method is the use of experimentally measured lattice distortion field as a source field for calculation of stress distribution in real semiconductors structure. Such a method allow us to solve important technical boundary value problems.

Acknowledgment
This research was supported by the State Committee for Scientific Research (KBN) in Poland under Grant No. 7 T07A 004 16.

References

[1] F. Speapen. Interfaces and stresses in thin films. *Acta Materialia*, **48**, 31–42, (2000).

[2] C Teodosiu. *Elastic Models of Crystal Defects*. Springer-Verlag and Editura Academiei, Berlin and Bucureşti, (1982).

[3] M. J. Hytch, E. Snoeck, and R. Kilaas. Quantitative measurement of displacement and strain fields from HTEM micrographs. *Ultramicroscopy*, **74**, 131–146, (1998).

[4] S. Kret, C. Delamarre, J. Y. Laval, and A. Dubon. Atomic-scale mapping of local lattice distortions in highly strained coherent islands of $In_xGa_{1-x}As$/GaAs by high-resolution electron microscopy and image processing. *Physical Review Letters*, **77**, 249–256, (1998).

[5] U. Stigh. A finite element study of threading dislocations. *Mechanics of Materials*, **14**(3), 179–187, (1993).

[6] S. Kret, P. Dłużewski, P. Dłużewski, C. Delamarre, A. Dubon, and J. Y. Laval. On the measurement of dislocation cores distribution in GaAs/ZnTe/CdTe. Submitted to publication, (2000).

[7] J. P. Hirth and J. Lothe. *Theory of Dislocations*. Wiley, New York, (1982).

[8] P. Dłużewski. *Continuum Theory of Dislocations as a Theory of Constitutive Modelling of Finite Elastic-Plastic Deformations*. Habilitation Thesis. IFTR Reports 13/1996, Warsaw, (1996).

[9] P. Dłużewski. On geometry and continuum thermodynamics of structural defect movement. *Mechanics of Materials*, **22**(1), 23–41, (1996).

[10] P. Dłużewski. Anisotropic hyperelasticity based upon general strain. Accepted for publication in *J. Elasticity*, (March, 2001).

[11] P. Dłużewski, G. Jurczak, and H. Antúnez. Anisotropic hyper-elastic finite element based upon generalized strain. In *This Conference*, (2001).

[12] R. W. Ogden. *Non-Linear Elastic Deformations*. Ellis Horwood Ltd., Chichester, (1984).

[13] K. Brugger. Thermodynamic definition of higher order elastic coefficients. *Physical Review*, **133**(6A), 1611–12, (1964).

[14] R. N. Thurston and K. Brugger. Third-order elastic constants and the velocity of small amplitude elastic waves in homogeneously stressed media. *Physical Review*, **133**(6A), 1604–10, (1964).

[15] N. J. Walker, G. A. Saunders, and J. E. Hawkey. Soft TA nodes and anharmonicity in cadmium telluride. *Philosophical Magazine B-Physics of Condensed Matter Structural Electronic Optical and Magnetic Properties*, **52**(5), 1005–1018, (1985).

[16] J. R. Drabble and A. J. Brammer. *Solid State Communications*, **4**(5), 467, (1966).

[17] P. Dłużewski and H. Antúnez. Finite element simulation of dislocation field movement. *Computer Assisted Mechanics and Engineering Science*, **2**, 141–148, (1995).

[18] P. Dłużewski and P. Rodzik. Elastic eigenstates in finite element modelling of large hyperelastic deformations. *Computer Methods in Applied Mechanics and Engineering*, **160**(3-4), 325–335, (1998).